Letter

Dynamically emergent correlations between particles in a switching harmonic trap

Marco Biroli [1], Manas Kulkarni [2], Satya N. Majumdar [1], and Grégory Schehr [3]

[1] *LPTMS, CNRS, Univ. Paris-Sud, Université Paris-Saclay, 91405 Orsay, France*

[2] *ICTS, Tata Institute of Fundamental Research, Bengaluru 560089, India*

[3] *Sorbonne Université, Laboratoire de Physique Théorique et Hautes Energies, CNRS UMR 7589, 4 Place Jussieu, 75252 Paris Cedex 05, France*

(Received 7 December 2023; accepted 9 February 2024; published 11 March 2024)

We study a one dimensional gas of N noninteracting diffusing particles in a harmonic trap, whose stiffness switches between two values μ_1 and μ_2 with constant rates r_1 and r_2, respectively. Despite the absence of direct interaction between the particles, we show that strong correlations between them emerge in the stationary state at long times, induced purely by the dynamics itself. We compute exactly the joint distribution of the positions of the particles in the stationary state, which allows us to compute several physical observables analytically. In particular, we show that the extreme value statistics (EVS), i.e., the distribution of the position of the rightmost particle, has a nontrivial shape in the large N limit. The scaling function characterizing this EVS has a finite support with a tunable shape (by varying the parameters). Remarkably, this scaling function turns out to be universal. First, it also describes the distribution of the position of the kth rightmost particle in a $1d$ trap. Moreover, the distribution of the position of the particle farthest from the center of the harmonic trap in d dimensions is also described by the same scaling function for all $d \geqslant 1$. Numerical simulations are in excellent agreement with our analytical predictions.

DOI: 10.1103/PhysRevE.109.L032106

Introduction. Stochastic resetting (SR) has emerged as a major area of research in statistical physics with multidisciplinary applications across diverse fields, such as search algorithms in computer science, foraging processes in ecology, reaction-diffusion processes in chemistry, and transcription processes in biology [1–3]. SR simply means interrupting the natural dynamics of a system at random times and instantaneously restarting the process either from its initial configuration or more generally from any predecided state. The interval between two successive resettings is typically Poissonian, though other protocols such as periodic resetting have also been studied. One of the main effects of SR is that the resetting moves violate detailed balance and drive the system to a nonequilibrium stationary state (NESS) [4,5]. Characterizing such a NESS and its possible spatial structure has generated a lot of interest, both theoretically (for reviews see [1–3]) and experimentally [6–9]. One of the simplest theoretical models corresponds to a single diffusing particle in d dimensions and subjected to SR with a constant rate r (i.e., Poissonian resetting) [4,5]. In this case, the position distribution becomes time independent at long times and has a nontrivial non-Gaussian shape. This result has been verified experimentally in optical traps setups [6]. Subsequently, several other models of single particle noisy dynamics subject to stochastic resetting have been studied theoretically [10–37].

The stochastic resetting for single particle systems discussed above can be easily generalized to many-body systems. In this case, the whole configuration of the system (i.e., all the degrees of freedom) is reset instantaneously to a predecided configuration at random times with rate r. This leads to a many-body NESS with interesting spatial structures that have been observed in a number of systems, such as fluctuating interfaces [38], symmetric exclusion process [39], the Ising model [40], etc. Recently, a very simple model of N noninteracting Brownian motions in one dimension, subjected to simultaneous resetting to their initial positions with rate r, was introduced [41]. Remarkably, even though the particles are noninteracting in this model, the simultaneous resetting generates an effective all-to-all attractive interaction between these particles that persists even at long times in the NESS. This model demonstrated an important phenomenon, namely the emergence of strong collective correlations in the steady state of a many-body system, where the interactions between constituents are not built in but instead emerge from the dynamics itself.

One of the shortcomings of these theoretical models, either for single or multiparticle systems, is the assumption of instantaneous resetting [15,26,27,42,43]. While this assumption makes the problem simpler and easier to implement in both numerical simulations and theoretical analysis, it is not very realistic experimentally. For example, in the optical trap experiments of a single diffusing particle with SR, the typical protocol consists of alternative intervals of free diffusion and confined motions [7,8]. During the free period, the particle is allowed to diffuse freely in the absence of an optical trap. At the end of this period a harmonic trap is switched on and the particle is thermally equilibrated in the trap. Once the particle has equilibrated, the trap is switched off and a new period of free motion starts. In the confined phase, no measurement is performed, since this protocol was designed to mimic the instantaneous resetting move [7,8]. One may naturally wonder what happens if one does not wait till the full equilibration in the confined phase but instead switches off the trap at a random time, e.g., distributed exponentially.

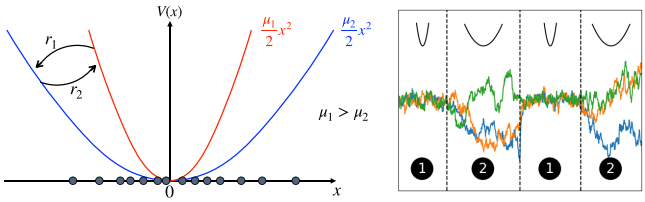

FIG. 1. The left panel illustrates the setup where N particles are confined in a harmonic potential $V(x)$, whose stiffness alternates between μ_1 and μ_2 with rates r_1 (from μ_1 to μ_2) and r_2 (from μ_2 to μ_1), respectively. On the right, we show the schematic trajectories for $N = 3$ diffusing particles. The switching times are shown by dashed vertical black lines.

This leads to a more realistic and general protocol where the particle moves in a harmonic trap whose stiffness switches intermittently between μ_1 and μ_2 (with $\mu_1 > \mu_2$ without any loss of generality). The stiffness changes from μ_1 to μ_2 with rate r_1 and reciprocally with rate r_2 from μ_2 to μ_1 (see Fig. 1 for an illustration). In the limit $\mu_1 \to \infty$, $\mu_2 \to 0$ with r_1 and r_2 fixed and subsequently $r_1 \to \infty$, this general protocol reduces to the standard model of diffusion under SR to the origin. The limit $\mu_1 \to \infty$ and $\mu_2 \to 0$ ensures resetting of a diffusing particle to the origin, while the subsequent limit $r_1 \to \infty$ guarantees that once it is reset to the origin, it immediately restarts, thus realizing the instantaneous resetting. For a single particle undergoing this switching intermittent protocol, the resulting position distribution in the NESS has been studied only recently, both theoretically [44–50] and experimentally in the $\mu_1 \to \infty$ limit [9]. In this paper, our goal is to study N independent particles undergoing this switching intermittent protocol. One of our main results is to show that, indeed, the switching dynamics between two stiffnesses of the trap drives the system into a NESS with strong collective correlations that emerge purely out of the dynamics. Thus, the emergence of strong correlations without direct interaction is a robust phenomenon and is not just an artefact of instantaneous resetting.

Let us first summarize our main results. For N independent particles on the line driven by this switching intermittent protocol, we first provide a complete characterization of the NESS, i.e., the exact computation of the joint distribution of the positions of the particles. This allows us to compute the spatial correlations in the NESS, as well as several other physical observables, such as the average density, the distribution of the position of the rightmost particle in the gas (extreme value statistics), the spacing distribution between particles and the full counting statistics (FCS), i.e., the statistics of the number of particles in a given interval. These observables have been calculated recently for large N in the limit of instantaneous resetting [41] but, here, we show that these asymptotic results get drastically modified under this intermittent switching protocol. In particular, we find a surprising result for the extreme value statistics (EVS), i.e., the distribution of the position M_1 of the rightmost particle. We show that in the large N limit, M_1 typically scales as $\sqrt{\ln N}$ and its probability distribution function (PDF) takes the scaling form

$$\text{Prob.}(M_1 = w, N) \approx \sqrt{\frac{r_H}{4D\,\ln N}}\, f\left(w\sqrt{\frac{r_H}{4D\,\ln N}}\right), \qquad (1)$$

where $r_H = 2/(1/r_1 + 1/r_2)$ is the harmonic mean of the switching rates and the scaling function $f(z)$ has a nontrivial shape supported over a finite interval $\sqrt{r_H/(2\mu_1)} \leqslant z \leqslant \sqrt{r_H/(2\mu_2)}$ [see Eqs. (16) and (17) and Fig. 2], even though the average density is supported over the full line (see Fig. 1). By tuning the parameters r_1, r_2, μ_1, μ_2, the shape of this PDF changes drastically as seen in Fig. 2. This is remarkable since in all the known examples of EVS in uncorrelated [51–58] or correlated [59–66] systems (for a recent review see [67]), including the instantaneous resetting case discussed above, the limiting distribution of the maximum is always supported over an unbounded interval (infinite or semiinfinite). The emergence of a finite support with a tunable shape for the EVS is thus a strong signature of the noninstantaneous nature of this switching protocol. In addition to having a finite support, we find that the scaling function $f(z)$ in Eq. (1) is surprisingly robust and universal: it also describes the scaling of the kth maximum in $d = 1$ as well as the distribution of the distance of the farthest particle from the center of a d-dimensional harmonic trap. In the rest of the paper, we present only the computation of the joint distribution and the EVS in Eq. (1). The computations of the other observables mentioned above are provided in the Supplemental Material [68].

The Model. We consider N independent Brownian particles on a line, all starting at the origin which feel a potential that switches between $V_1(x) = \mu_1 x^2/2$ and $V_2(x) = \mu_2 x^2/2$, with Poissonian rate r_1 (from μ_1 to μ_2) and rate r_2 (from μ_2 to μ_1). Hence, the duration τ of the time intervals between successive switches is distributed via $\text{Prob.}[\tau] = r_i e^{-r_i \tau}$, where r_i is r_1 or r_2. Moreover, the intervals are statistically independent. In each phase the positions $\{x_i\}$ evolve as independent Ornstein-Uhlenbeck processes [78]

$$\frac{dx_i}{dt} = -\mu_k x_i + \sqrt{2D}\eta_i(t), \qquad (2)$$

where $\mu_k = \mu_1$ or μ_2 depending on the phase, D is the diffusion constant and $\eta_i(t)$ is a zero-mean Gaussian white noise with a correlator $\langle \eta_i(t)\eta_j(t')\rangle = \delta_{ij}\delta(t - t')$. Let $P_1(\vec{x}, t)$ (resp. P_2) denote the joint PDF of the particles being at $\vec{x} = (x_1, \ldots, x_N)$ at time t and that the system is in phase 1 (resp. phase 2). From Eq. (2), they evolve by the coupled Fokker-Planck equations

$$\frac{\partial P_1}{\partial t} = \sum_{i=1}^{N}\left[D\frac{\partial^2 P_1}{\partial x_i^2} + \mu_1 \frac{\partial}{\partial x_i}(x_i P_1)\right] - r_1 P_1 + r_2 P_2 \qquad (3)$$

$$\frac{\partial P_2}{\partial t} = \sum_{i=1}^{N}\left[D\frac{\partial^2 P_2}{\partial x_i^2} + \mu_2 \frac{\partial}{\partial x_i}(x_i P_2)\right] - r_2 P_2 + r_1 P_1 \qquad (4)$$

with the initial conditions

$$P_1(\vec{x}, t = 0) = \tfrac{1}{2}\delta(\vec{x}) \quad \text{and} \quad P_2(\vec{x}, t = 0) = \tfrac{1}{2}\delta(\vec{x}), \qquad (5)$$

where we assumed that, initially, both phases occur equally likely. Hence, the joint PDF of the positions only is given by $P(\vec{x}, t) = P_1(\vec{x}, t) + P_2(\vec{x}, t)$. The first terms on the right hand side of Eqs. (3) and (4) represent diffusion and advection in a harmonic potential, while the last two terms represent the loss and gain due to the switching between potentials, with rates r_1 and r_2, respectively. Note that Eqs. (3) and (4) also describe the motion of N components of a single particle in N spatial

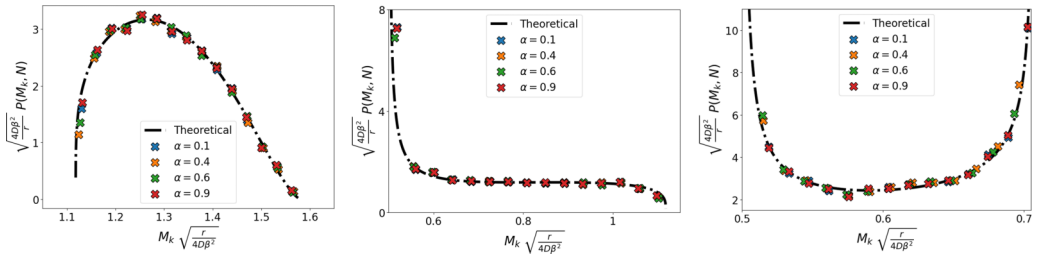

FIG. 2. Scaling collapse of the distribution of the kth maximum as in Eq. (17) for different values of $\alpha = k/N$ and different values of the parameters. We set $r_1 = r_2 = 1$, $D = 1$, $N = 10^6$, and vary μ_1 and μ_2. From left to right we used, respectively, $\mu_1 = 0.4$, $\mu_2 = 0.2$, then $\mu_1 = 2$, $\mu_2 = 0.4$, and finally $\mu_1 = 2$, $\mu_2 = 1$. The dashed black line corresponds to the theoretical prediction and the symbols are the numerical results. Different colors correspond to different values of α. The numerical results were obtained by sampling 10^5 examples directly from the NESS distribution given in Eq. (12).

dimensions in a switching harmonic trap. However, here we consider them as the positions of N independent particles in a gas that allows us to study observables with physical meaning only in the latter interpretation, such as gap statistics or the full counting statistics, etc.

To solve this pair of Fokker-Planck equations, it is convenient to work in the Fourier space where we define $\tilde{P}_n(\vec{k}, t) = \int_{-\infty}^{+\infty} d\vec{x}\, e^{i\vec{k}x} P_n(\vec{x}, t)$, with $n = 1, 2$. In the steady state, setting $\partial_t \tilde{P}_n = 0$, Eqs. (3) and (4) in the Fourier space reduce to

$$\left(D\sum_{i=1}^{N} k_i^2 + r_1\right)\tilde{P}_1 + \mu_1 \sum_{i=1}^{N} k_i \frac{\partial \tilde{P}_1}{\partial k_i} = r_2 \tilde{P}_2, \tag{6}$$

$$\left(D\sum_{i=1}^{N} k_i^2 + r_2\right)\tilde{P}_2 + \mu_2 \sum_{i=1}^{N} k_i \frac{\partial \tilde{P}_2}{\partial k_i} = r_1 \tilde{P}_1, \tag{7}$$

with initial conditions $\tilde{P}_n(\vec{k} = 0) = 1/2$. Notice that Eqs. (6) and (7) are spherically symmetric. It is therefore much easier to move to hyperspherical coordinates where $k = \sqrt{\sum_{i=1}^{N} k_i^2}$ is the distance to the origin and θ_i, for $i = 1, \cdots, N-1$ are the different angular coordinates. Then Eqs. (6) and (7) simplify to

$$[(Dk^2 + r_1) + \mu_1 k \partial_k]\tilde{P}_1 = r_2 \tilde{P}_2, \tag{8}$$

$$[(Dk^2 + r_2) + \mu_2 k \partial_k]\tilde{P}_2 = r_1 \tilde{P}_1. \tag{9}$$

Notice that by permuting the indices $1 \leftrightarrow 2$ in Eq. (8) leads to Eq. (9). Hence, we can solve only for $\tilde{P}_1$ and the solution for $\tilde{P}_2$ will follow by permuting the indices. By eliminating $\tilde{P}_2$ between Eqs. (8) and (9) we get an ordinary second order differential equation for $\tilde{P}_1$ (respectively $\tilde{P}_2$). Solving these ordinary differential equations with appropriate boundary conditions (see the Supplemental Material for details), we obtain

$$\tilde{P}_1(k) = \frac{r_2\, e^{-\frac{Dk^2}{2\mu_1}}}{r_1 + r_2} M\left(R_1; 1 + R_1 + R_2; \frac{Dk^2(\mu_2 - \mu_1)}{2\mu_1\mu_2}\right), \tag{10}$$

where $R_1 = r_1/(2\mu_1)$, $R_2 = r_2/(2\mu_2)$, and $M(a; b; z)$ is the Kummer's function [79]. Similarly, one can obtain $\tilde{P}_2(\vec{k})$ just by exchanging $\mu_1 \leftrightarrow \mu_2$ and $r_1 \leftrightarrow r_2$. To reveal the spatial correlations in the NESS, it is useful to invert this Fourier transform, which is not easy. However, fortunately, one can make use of a convenient integral representation [79]

$$M(a; b; z) = \frac{\Gamma(b)}{\Gamma(a)\Gamma(b-a)} \int_0^1 du\, e^{zu} u^{a-1}(1-u)^{b-a-1}, \tag{11}$$

where $\Gamma(x)$ is the Γ function. Using Eq. (11) in Eq. (10) and inverting the Fourier transform we obtain an expression for $P_1(\vec{x})$ and similarly for $P_2(\vec{x})$. Adding them gives the joint PDF in the NESS [68]

$$P^{\rm st}(\vec{x}) = \int_0^1 du\, h(u) \prod_{i=1}^{N} p(x_i|u), \tag{12}$$

where

$$h(u) = \frac{c\, r_H}{4} u^{R_1 - 1}(1-u)^{R_2 - 1}\left[\frac{1-u}{\mu_1} + \frac{u}{\mu_2}\right] \tag{13}$$

with $c = \Gamma(R_1 + R_2 + 1)/(\Gamma(R_1 + 1)\Gamma(R_2 + 1))$ and $r_H = 2\, r_1 r_2/(r_1 + r_2)$. The function $p(x|u) = e^{-\frac{x^2}{2V(u)}}/\sqrt{2\pi V(u)}$ is a pure Gaussian with zero mean and variance $V(u) = D(\frac{u}{\mu_2} + \frac{1-u}{\mu_1})$. This fully characterizes the joint PDF of the positions in the NESS. Note that $h(u)$ is normalized to unity, i.e., $\int_0^1 h(u)du = 1$. Thus, one can interpret Eq. (12) as the joint distribution of N i.i.d. Gaussian variables with zero mean and a common variance $V(u)$ parametrized by u, which itself is a random variable distributed via the PDF $h(u)$. There is indeed a nice physical meaning of this random variable u. If the particle was entirely in phase 2, its stationary distribution would be a Gaussian (the Gibbs state) with a variance D/μ_2. In contrast, if it was in phase 1, it will again be a Gaussian with a variance D/μ_1. Hence, from the formula $V(u) = D(\frac{u}{\mu_2} + \frac{1-u}{\mu_1})$, one sees that $0 \leqslant u \leqslant 1$ can be interpreted as the effective fraction of time that each particle spends in phase 2. This can be put on a more rigorous footing by using the so-called Kesten variables as shown in the Supplemental Material [68]. For simplicity, we will henceforth set $r_1 = r_2 = r$ and the results for general $r_1 \neq r_2$ are given in the Supplemental Material [68].

We note that the joint PDF in Eq. (12) does not factorize, indicating the presence of correlations in the NESS. One can easily calculate the two-point correlation function from Eq. (12) using the fact that, for a fixed u, they are i.i.d. variables. The natural correlator $\langle x_i x_j\rangle - \langle x_i\rangle\langle x_j\rangle$ for $i \neq j$ vanishes identically since $p(x_i|u)$ is Gaussian and hence symmetric in x_i. The first nonzero correlator for $i \neq j$ is

given by

$$\langle x_i^2 x_j^2\rangle - \langle x_i^2\rangle\langle x_j^2\rangle = \frac{D^2}{r^2}\frac{(R_1-R_2)^2(2+3R_1+3R_2+4R_1R_2)}{(1+R_1+R_2)^2(2+R_1+R_2)}, \tag{14}$$

where we recall that $R_1 = r/(2\mu_1)$ and $R_2 = r/(2\mu_2)$. The positive value of this correlator indicates that there are effective all-to-all attractive correlations between the particles in the NESS. These correlations are not built-in but get generated by the switching dynamics of the potential, which all the particles share together. This makes the particles strongly correlated in the NESS. Despite such strong correlations, the structure of the joint PDF in Eq. (12) allows us to compute several physical observables exactly, such as the average density, the EVS, the distribution of the spacings between particles and also the FCS. The reason for the solvability can be traced back to Eq. (12) where one can first fix u and compute the observables for N independent variables, each distributed via $p(x|u)$ where u is just a fixed parameter and then the average over u drawn from the PDF $h(u)$ in Eq. (13). For i.i.d. variables, this computation is rather standard. This solvable structure holds more generally for any conditionally independent and identically distributed (c.i.i.d.) variables, as studied recently in Ref. [80]. Here, the c.i.i.d. structure emerges from the basic dynamics of the system and thus provides a natural physical example of such systems. The computations of these physical observables are provided in detail in the Supplemental Material [68], and here we focus only on the EVS. This is because the EVS of strongly correlated variables is known to be a very hard problem and there are only a few cases where it can be derived analytically. Our model provides not only a solvable example of EVS in a strongly correlated system, but also the distribution of the EVS turns out to be rather surprising, as discussed below.

To compute the EVS, we start from the joint PDF in Eq. (12). We first fix u and compute the EVS of N i.i.d. Gaussian random variables of zero mean and variance $V(u)$. It is well known [67] that, for large N, the maximum M_1 of such i.i.d. Gaussian variables behaves almost deterministically as $M_1 \approx \sqrt{2V(u)\ln N}$, with fluctuations around it of order $1/\sqrt{\ln N}$. It turns out that, to leading order for large N, one can approximate this distribution by a delta function, namely $P(M_1 = w|u) \approx \delta(w - \sqrt{2V(u)\ln N})$. Finally, averaging over u we get

$$P(M_1 = w, N) \approx \int_0^1 \mathrm{d}u\, h(u)\, \delta(w - \sqrt{2V(u)\ln N}), \tag{15}$$

where $V(u) = D(u/\mu_2 + (1-u)/\mu_1)$ and $h(u)$ is given in Eq. (13). Performing this integral explicitly [68], we get the scaling form in Eq. (1) where the scaling function $f(z)$ has a nontrivial shape given by

$$f(z) = \frac{c\, R_1^{R_1-1} R_2^{R_2-1}}{(R_2-R_1)^{R_1+R_2-1}}|z|^3\left(1-\frac{z^2}{R_2}\right)^{R_2-1}\left(\frac{z^2}{R_1}-1\right)^{R_1-1}, \tag{16}$$

with $\sqrt{R_1} \leqslant z \leqslant \sqrt{R_2}$. As mentioned earlier, an EVS scaling function with a finite support is rather surprising because the average density is spread over the full real line [68]. Moreover, the shape of the scaling function $f(z)$ can be tuned by varying the parameters R_1 and R_2. At both edges of the support, $f(z)$ can either diverge, go to a nonzero constant, or vanish, depending on R_1, R_2. The scaling function $f(z)$ also turns out to be universal in the following sense. If one calculates the distribution of the kth maximum (order statistics), one finds a scaling form

$$\text{Prob.}[M_k = w, N] \approx \sqrt{\frac{r_H}{4D\beta^2}}\, f\left(w\sqrt{\frac{r_H}{4D\beta^2}}\right), \tag{17}$$

where $\beta = \mathrm{erfc}^{-1}(2k/N)$, but the scaling function $f(z)$ is independent of k and has the same expression as in Eq. (16). Here $\mathrm{erfc}(z) = 2/\sqrt{\pi}\int_z^\infty e^{-y^2}\,\mathrm{d}y$. In Fig. 2, we verify this scaling form by collapsing data for different $\alpha = k/N$ and for different values of R_1 and R_2. The numerical results are in excellent agreement with our theoretical predictions. Furthermore, one can easily generalize our results to a harmonic trap in d dimensions [68]. Following exactly the same analysis as in the $d = 1$ case above, one can also compute the distribution of the distance of the farthest particle from the center of the trap and we find the remarkable result that it is again described by Eq. (1) with the same scaling function $f(z)$ given in Eq. (16). Thus, the scaling function $f(z)$ is extremely robust and "super universal" in the sense that it neither depends on k in $d = 1$, nor on the dimension d itself.

To summarize, we have completely characterized the nonequilibrium stationary state of N Brownian particles in a harmonic trap in an experimentally realistic protocol where the stiffness of the trap switches between two values at constant rate. The strong correlations between the positions of the particles in the stationary state emerge from the dynamics itself and are not built in. The exact joint distribution of the particle positions allows us to compute several physical observables analytically. In particular, we have shown that the EVS is characterized by a nontrivial scaling function which has a finite support and a tunable shape. Moreover, the scaling function of the EVS is universal in the sense that it also describes the limiting distribution of the kth maximum in $d = 1$, as well as the distribution of the distance of the particle farthest from the center of the harmonic trap in d dimensions [68]. It would be interesting if our predictions could be verified experimentally and also to investigate the NESS in nonharmonic traps.

Acknowledgments. M.K. and S.N.M. would like to thank the Isaac Newton Institute for Mathematical Sciences, Cambridge, for support and hospitality during the programme "New statistical physics in living matter: nonequilibrium states under adaptive control" where work on this paper was undertaken. This work was supported by EPSRC Grant No. EP/R014604/1. M.K. would like to acknowledge support from the CEFIPRA Project 6004-1, SERB Matrics Grant No. (MTR/2019/001101), and SERB VAJRA faculty scheme (VJR/2019/000079). M.K. acknowledges support from the Department of Atomic Energy, Government of India, under Project No. RTI4001.

[1] M. R. Evans, S. N. Majumdar, and G. Schehr, J. Phys. A: Math. Theor. **53**, 193001 (2020).
[2] A. Pal, S. Kostinski, and S. Reuveni, J. Phys. A: Math. Theor. **55**, 021001 (2022).
[3] S. Gupta and A. M. Jayannavar, Front. Phys. **10**, 789097 (2022).
[4] M. R. Evans and S. N. Majumdar, Phys. Rev. Lett. **106**, 160601 (2011).
[5] M. R. Evans and S. N. Majumdar, J. Phys. A: Math. Theor. **44**, 435001 (2011).
[6] O. Tal-Friedman, A. Pal, A. Sekhon, S. Reuveni, and Y. Roichman, J. Phys. Chem. Lett. **11**, 7350 (2020).
[7] B. Besga, A. Bovon, A. Petrosyan, S. N. Majumdar, and S. Ciliberto, Phys. Rev. Res. **2**, 032029(R) (2020).
[8] F. Faisant, B. Besga, A. Petrosyan, S. Ciliberto, S. N. Majumdar, J. Stat. Mech. (2021) 113203.
[9] R. Goerlich, M. Li, L. B. Pires, P. A. Hervieux, G. Manfredi, C. Genet, arXiv:2306.09503.
[10] S. Reuveni, M. Urbakh, and J. Klafter, Proc. Natl. Acad. Sci. USA **111**, 4391 (2014).
[11] D. Boyer and C. Solis-Salas, Phys. Rev. Lett. **112**, 240601(R) (2014).
[12] T. Rotbart, S. Reuveni, and M. Urbakh, Phys. Rev. E **92**, 060101(R) (2015).
[13] S. N. Majumdar, S. Sabhapandit, and G. Schehr, Phys. Rev. E **92**, 052126 (2015).
[14] A. Pal, A. Kundu, and M. R. Evans, J. Phys. A: Math. Theor. **49**, 225001 (2016).
[15] S. Reuveni, Phys. Rev. Lett. **116**, 170601 (2016).
[16] M. Montero and J. Villarroel, Phys. Rev. E **94**, 032132 (2016).
[17] A. Nagar and S. Gupta, Phys. Rev. E **93**, 060102(R) (2016).
[18] A. Pal and S. Reuveni, Phys. Rev. Lett. **118**, 030603 (2017).
[19] D. Boyer, M. R. Evans, and S. N. Majumdar, J. Stat. Mech. (2017) 023208.
[20] M. R. Evans and S. N. Majumdar, J. Phys. A: Math. Theor. **51**, 475003 (2018).
[21] A. Chechkin and I. M. Sokolov, Phys. Rev. Lett. **121**, 050601 (2018).
[22] G. Mercado-Vasquez and D. Boyer, J. Phys. A: Math. Theor. **51**, 405601 (2018).
[23] A. Pal, L. Kuśmierz, and S. Reuveni, Phys. Rev. E **100**, 040101(R) (2019).
[24] A. Masó-Puigdellosas, D. Campos, and V. Méndez, Front. Phys. **7**, 112 (2019).
[25] A. Pal, L. Kusmierz, and S. Reuveni, Phys. Rev. Res. **2**, 043174 (2020).
[26] A. S. Bodrova and I. M. Sokolov, Phys. Rev. E **101**, 052130 (2020).
[27] A. S. Bodrova and I. M. Sokolov, Phys. Rev. E **102**, 032129 (2020).
[28] B. De Bruyne, J. Randon-Furling, and S. Redner, Phys. Rev. Lett. **125**, 050602 (2020).
[29] P. C. Bressloff, J. Phys. A: Math. Theor. **53**, 425001 (2020).
[30] R. G. Pinsky, Stoch. Proc. Appl. **130**, 2954 (2020).
[31] V. Stojkoski, T. Sandev, L. Kocarev, and A. Pal, Phys. Rev. E **104**, 014121 (2021).
[32] B. De Bruyne, S. N. Majumdar, and G. Schehr, Phys. Rev. Lett. **128**, 200603 (2022).
[33] F. Mori, S. N. Majumdar, and G. Schehr, Phys. Rev. E **106**, 054110 (2022).
[34] I. Santra, U. Basu, and S. Sabhapandit, J. Phys. A: Math. Theor. **55**, 414002 (2022).
[35] B. De Bruyne and F. Mori, Phys. Rev. Res. **5**, 013122 (2023).
[36] M. Biroli, S. N. Majumdar, and G. Schehr, Phys. Rev. E **107**, 064141 (2023).
[37] F. Mori, K. S. Olsen, and S. Krishnamurthy, Phys. Rev. Res. **5**, 023103 (2023).
[38] S. Gupta, S. N. Majumdar, and G. Schehr, Phys. Rev. Lett. **112**, 220601 (2014).
[39] U. Basu, A. Kundu, and A. Pal, Phys. Rev. E **100**, 032136 (2019).
[40] M. Magoni, S. N. Majumdar, and G. Schehr, Phys. Rev. Res. **2**, 033182 (2020).
[41] M. Biroli, H. Larralde, S. N. Majumdar, and G. Schehr, Phys. Rev. Lett. **130**, 207101 (2023).
[42] M. R. Evans and S. N. Majumdar, J. Phys. A: Math. Theor. **52**, 01LT01 (2019).
[43] J. C. Sunil, R. A. Blythe, M. R. Evans, and S. N. Majumdar, J. Phys. A: Math. Theor. **56**, 395001 (2023).
[44] G. Mercado-Vasquez, D. Boyer, S. N. Majumdar, G. Schehr, J. Stat. Mech. (2020) 113203.
[45] D. Gupta, C. A. Plata, A. Kundu, and A. Pal, J. Phys. A: Math. Theor. **54**, 025003 (2021).
[46] I. Santra, S. Das, and S. K. Nath, J. Phys. A: Math. Theor. **54**, 334001 (2021).
[47] P. Xu, T. Zhou, R. Metzler, and W. Deng, New J. Phys. **24**, 033003 (2022).
[48] D. Gupta and C. A. Plata, New J. Phys. **24**, 113034 (2022).
[49] H. Alston, L. Cocconi, and T. Bertrand, J. Phys. A: Math. Theor. **55**, 274004 (2022).
[50] G. Mercado-Vàsquez, D. Boyer, S. N. Majumdar, J. Stat. Mech. (2022) 093202.
[51] E. J. Gumbel, *Statistics of Extremes* (Dover, New York, 1958).
[52] C. W. Anderson, J. R. Statist. Soc. B **40**, 197 (1978).
[53] M. R. Leadbetter, G. Lindgren, and H. Rootzen, *Extremes and Related Properties of Random Sequences and Processes* (Springer-Verlag, New York, 1982).
[54] B. Derrida, J. Phys. Lett. **46**, 401 (1985).
[55] I. Weissman, Adv. Appl. Probab. **20**, 8 (1988).
[56] B. C. Arnold, N. Balakrishnan, and H. N. Nagaraja, *A First Course in Order Statistics* (Wiley, New York, 1992).
[57] H. N. Nagaraja and H. A. David, *Order Statistics (Third Ed.)* (Wiley, New Jersey, 2003).
[58] J. Y. Fortin and M. Clusel, J. Phys. A: Math. Theor. **48**, 183001 (2015).
[59] C. A. Tracy and H. Widom, Commun. Math. Phys. **159**, 151 (1994).
[60] D. Carpentier and P. Le Doussal, Phys. Rev. E **63**, 026110 (2001).
[61] D. S. Dean and S. N. Majumdar, Phys. Rev. E **64**, 046121 (2001).
[62] S. N. Majumdar and P. L. Krapivsky, Physica A **318**, 161 (2003).
[63] S. N. Majumdar and A. Comtet, Phys. Rev. Lett. **92**, 225501 (2004).
[64] S. N. Majumdar and A. Comtet, J. Stat. Phys. **119**, 777 (2005).
[65] G. Schehr and S. N. Majumdar, Phys. Rev. E **73**, 056103 (2006).
[66] E. Bertin and M. Clusel, J. Phys. A: Math. Gen. **39**, 7607 (2006).

[67] S. N. Majumdar, A. Pal, and G. Schehr, Phys. Rep. **840**, 1 (2020).
[68] See Supplemental Material at http://link.aps.org/supplemental/10.1103/PhysRevE.109.L032106 for detailed derivations of the results presented in the main letter, which also includes [69–77].
[69] H. Kesten, Acta Math. **131**, 207 (1973).
[70] H. Kesten, M. V. Kozlov, and F. Spitzer, Compos. Math. **30**, 145 (1975).
[71] B. Derrida and H. J. Hilhorst, J. Phys. A: Math. Gen. **16**, 2641 (1983).
[72] H. Kesten and F. Spitzer, Z. Wahrscheinlichkeit **67**, 363 (1984).
[73] C. de Calan, J. M. Luck, T. M. Nieuwenhuizen, and D. Petritis, J. Phys. A **18**, 501 (1985).
[74] C. M. Goldie, Ann. Appl. Probab. **1**, 126 (1991).
[75] D. Buraczewski, E. Damek, T. Mikosch, and J. Zienkiewicz, Ann. Probab. **41**, 2755 (2013).
[76] T. Gautié, J.-P. Bouchaud, P. Le Doussal, J. Phys. A: Math. Theor. **54**, 255201 (2021).
[77] M. Guéneau, S. N. Majumdar, and G. Schehr, J. Phys. A: Math. Theor. **56**, 475002 (2023).
[78] G. E. Uhlenbeck and L. S. Ornstein, Phys. Rev. **36**, 823 (1930).
[79] F. W. J. Olver, D. W. Lozier, R. F. Boisvert, and C. W. Clark, *The NIST Handbook of Mathematical Functions* (Cambridge University Press, New York, 2010).
[80] M. Biroli, H. Larralde, S. N. Majumdar, and G. Schehr, Phys. Rev. E **109**, 014101 (2024).